Robotica (2016) volume 34, pp. 468–481. © Cambridge University Press 2014
doi:10.1017/S0263574714001799

Study on hexapod robot manipulation using legs

Xilun Ding and Fan Yang*

Robotics Research Institute, Beihang University, Haidian District, Beijing, China

(Accepted Jun 9, 2014. First published online: July 9, 2014)

SUMMARY

In order to provide a novel approach for the operational problems of walking robots, this paper presents a method by which a hexapod robot uses its legs to manipulate an object, and this involves the following two steps. First, two adjacent legs are used to manipulate the object. Next, the supporting legs are required to assist the arms to obtain high manipulability. The manipulation constraints, workplaces, and kinematic models are analyzed using screw theories. Moreover, an optimization algorithm is proposed to reduce energy consumption under stability constraints. We also introduce a manipulation control model that simultaneously considers the supporting and operating legs. Finally, the validity of these methods is proved by the results of experiments and simulations.

KEYWORDS: Manipulation; Hexapod robot; Kinematic analysis.

1. Introduction

Multi-legged robots display significant advantages with respect to wheeled ones for walking over rough terrain because they do not require continuous contact with the ground.[1] Among the multi-legged robots, hexapod robots have the highest efficiency for statically stable walking. Preumount *et al*.[2] observed that more than six legs does not increase the walking speed. Hexapod robots also exhibit robustness in the case of leg faults and make it possible for the robot to use one, two, or three legs to function as hands.[3,4] For these reasons, hexapod robots have become an intensive research topic in recent years, with the research studies primarily focusing on gait and locomotion planning, which today has reached, to some extent, a state of maturity.

Concurrently, hexapod robots are being studied to address the requirements from real applications, which indicate that manipulation plays as important role as locomotion. The first notable prototype developed for object manipulation was a mobile manipulator;[5,6] this mobile manipulator prototype consists of a manipulator arm mounted onto a mobile base. The mobile manipulator exhibits dexterous manipulation with fast and precise movement capability. Typically, the base and the arm are treated disjointly. The mobile base used can be wheeled, tracked, or legged. The arms are heavy burdens for the robot base and may have negative effects on moving stability. A method adopted to overcome these problems is to utilize legs with various end-effectors. Kato and Hirose[7] developed a quadruped robot named TITAN-IX, which exhibited a high working performance. Particular end-effectors are equipped according to various tasks via a tool changing system located on its back. ATHLETE,[8,9] well known as the most advanced hexapod robot developed for lunar exploration, has a quick-disconnect tool adapter located on each wheel, it can be used to extract any sort of tool from a "holster." Due to the complexity and precision of end-effectors, a protection method should be considered, and the tool changing system must provide a sufficient selection of end-effectors to accomplish various tasks. Inspired by the observation that insects can dexterously use their limbs for manipulation and locomotion, Koyachi *et al.*[10,11] proposed the definition of a "limb mechanism." A limb mechanism has multiple limbs comprising links and kinematic pairs, which interface the body of a robot with its environment. A robot with limb mechanisms can execute tasks dexterously and can move quickly on uneven or rather rough terrain. To validate this concept, a prototype named MELMANTIS-I[12] was developed, and the control method was also presented. However, the arm and leg mechanisms

* Corresponding author: E-mail: robot.fan@me.buaa.edu.cn

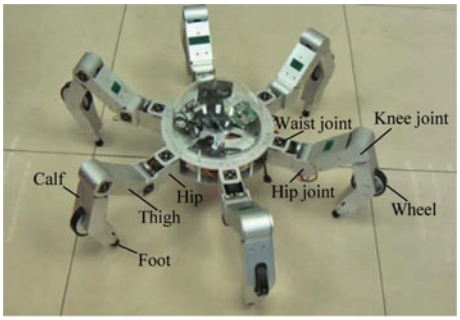

(a) Robot

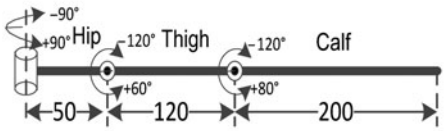

(b) Leg

Fig. 1. NOROS-III robot structure: (a) robot, (b) leg.

have their own, and sometimes conflicting, characteristics, making it difficult to design a simple and effective mechanism that integrates arm and leg functions as a whole.

Some recent studies for improving the manipulability of mobile robots are mainly embodied on humanoid robots. Inoue *et al.*[13] proposed a method for adjusting leg motion for the improvement of arm's manipulability. Bouyarmane and Kheddar[14] considered the multi-contact sequences of manipulation that allow the humanoid robot to realize different tasks. Tumble stability[15] was also proposed for integrated locomotion and manipulation. An excellent work describing novel hexapod robot design and providing a summary of recent control methods was presented by Melaka.[16] The use of biologically inspired control is a main trend for recent hexapod robot studies.[17,18] Inoue *et al.*[19] recently proposed three control methods of pushing objects for a novel hexapod robot. Voyles and Larson[20] developed a novel embedded within joint force sensor for precise control of grasping.

While examining the present state of the art, most of the present methods for improving mobile robots' manipulability were found to rely heavily on particular designed mechanisms, such as various end effectors, additional manipulators, and limb mechanisms. A general control method does not appear to have been published. This paper presents a new manipulation method for hexapod robots that is mainly inspired by the coordinated grasp method of a multi-fingered hand robot. These manipulation methods are intuitively organized into two steps. First, the robot uses two adjacent legs as arms to manipulate an object; this method is simple and effective for small-range operations, similar to the manner in which people use hands to grasp a cup of water. Next, the remaining four supporting legs are required to assist the two legs performing object manipulation by adjusting the postures of the body via bending and stretching. The proposed method enables a larger operating range, similar to how people stoop down to pick up a box at a distance. As the structure dimension is parameterized during the analysis, the proposed method can be applied to a wide range of hexapod robots.

The paper is organized as follows: In Section 2, the structures of the Novel Robotics System for Planetary Exploration III (NOROS-III) robot are described; Section 3 introduces two methods for integrated arm and leg manipulations; simulations and experiments are presented in Section 4; finally, conclusions are drawn in Section 5.

2. Structure of NOROS-III robot

The NOROS-III robot, shown in Fig. 1(a), is being developed for lunar exploration. The robot is 980 mm in width, 120 mm in height (millimeter is used as the length unit in this paper unless

https://doi.org/10.1017/S0263574714001799 Published online by Cambridge University Press

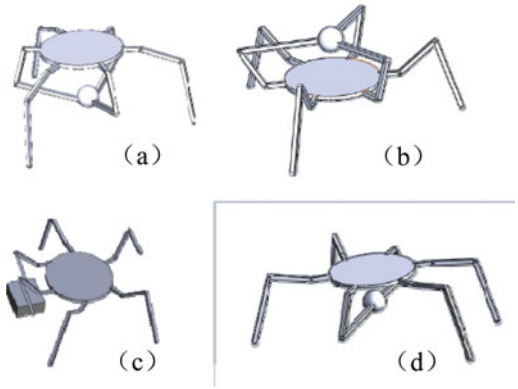

Fig. 2. Schematic diagrams of hexapod manipulation.

otherwise noted) with six wheel-legs distributed axisymmetrically around the body, which provides omni-directional mobility. Each leg consists of three revolute joints, the design parameters of which are shown in Fig. 1(b). The hybrid locomotion system allows motion by legs to cross a highly soft or rough terrain and can achieve a maximum speed of 3 km/h by moving on wheels when hard smooth surfaces are encountered.[21] The weight of the robot is approximately 4 kg, including that of mechanical components, control system, and lithium batteries. The robot is equipped with different sensors for various tasks. The normal force applied to the leg tip is measured by using a 1-degree-of-freedom (DOF) force sensor. Obstacles are sensed by fusing the data obtained from a web-camera and six infrared sensors. Remote control commands and the video signal from the camera are transmitted through wireless LAN, which enable the robot to remotely perform various tasks in hazardous environments.

3. Integrated arm and leg manipulation methods

There are at least three legs required for maintaining static stability, while other legs can be used for manipulation; thus, the integrated arm and leg manipulation can be categorized by which legs are used for manipulation. Some schemes of the manipulation are sketched in Fig. 2.

Figures 2(a) and (b) show the operation using three legs, with the workspaces located below and above the body respectively. These manipulation methods exhibit higher accuracy and stability; however, the workspace is smaller, and the scale of the target objects is limited.

Figures 2(c) and (d) show the operation using two adjacent and opposite legs respectively. These methods enable a larger workspace and a greater range of target objects at the expense of lower operation accuracy and stability. Note that the method depicted in Fig. 2(d) is especially suited for transportation operations. In this paper, we consider the method illustrated in Fig. 2(c) because of the larger workspace for object manipulation.

3.1. Kinematic analysis of the basic manipulation method

The basic manipulation method discussed in this section is a simple and effective way to pick or place some objects that involves the use of two adjacent legs of a hexapod robot while the other four supporting legs do not move. This situation can be considered the manipulation of a dual-arm robot. According to the simplified contact model,[22] we suppose that all contacts between the leg tips and the object are idealized as point contacts at fixed locations. This simplification allows one to ignore the possibility that a leg tip rolls or slides along the surface of the object.[23] In this case, the body, legs, and the object form a closed kinematic chain in which the target object is regarded as the mobile platform, and the body is regarded as the fixed platform. The body coordinate frame Σ_R and the object coordinate frame Σ_o are fixed on the body center and the target object center separately. We analyze the kinematic relation by using screw theories, with the initial manipulation configuration set symmetrically along X-axis in Z = 0 plane and the dimensions of the structure symbolized as shown in Fig. 3.

https://doi.org/10.1017/S0263574714001799 Published online by Cambridge University Press

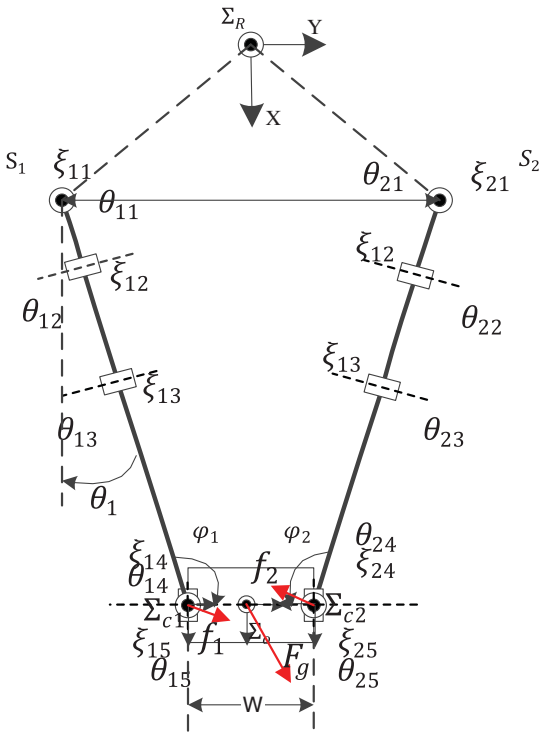

Fig. 3. Coordinate frames and parameters.

According to the product of exponentials formula, the structure equation is described as follows:

$$\begin{cases} g_{\mathrm{OB}}(\theta) = \mathrm{e}^{\hat{\xi}_{11}\theta_{11}}\mathrm{e}^{\hat{\xi}_{12}\theta_{12}}\mathrm{e}^{\hat{\xi}_{13}\theta_{13}}\mathrm{e}^{\hat{\xi}_{14}\theta_{14}}\mathrm{e}^{\hat{\xi}_{15}\theta_{15}}g_{\mathrm{OB}}(0) \\ g_{\mathrm{OB}}(\theta) = \mathrm{e}^{\hat{\xi}_{21}\theta_{21}}\mathrm{e}^{\hat{\xi}_{22}\theta_{22}}\mathrm{e}^{\hat{\xi}_{23}\theta_{23}}\mathrm{e}^{\hat{\xi}_{24}\theta_{24}}\mathrm{e}^{\hat{\xi}_{25}\theta_{25}}g_{\mathrm{OB}}(0) \end{cases}, \tag{1}$$

where $g_{\mathrm{OB}}(\theta)$ is the final configuration of the object with joint angles θ, and $g_{\mathrm{OB}}(0)$ is the initial configuration of the object.

No collisions should occur between the two legs because of joint configurations and kinematic constraints. The conditions for avoiding collisions between the legs and the object (convex polyhedron) can be denoted as

$$\begin{cases} \emptyset_1 > 90^\circ \\ \emptyset_2 > 90^\circ \end{cases}, \tag{2}$$

where $\emptyset_i$ is the space angle contained by Leg_i and the object.

Any physical leg will have limits on the torque that can be exerted at each of the leg joints. These limits can be described by the following formula:

$$\tau = J_h^T f_c \leq \tau_{\max}, \tag{3}$$

where J_h is the Jacobian matrix for the leg, and f_c represents the leg contact forces and moments that are described by the 6×1 generalized force vector. An important property of a grasp is the ability to balance external object wrenches by applying appropriate leg wrenches at the contact points, also

https://doi.org/10.1017/S0263574714001799 Published online by Cambridge University Press

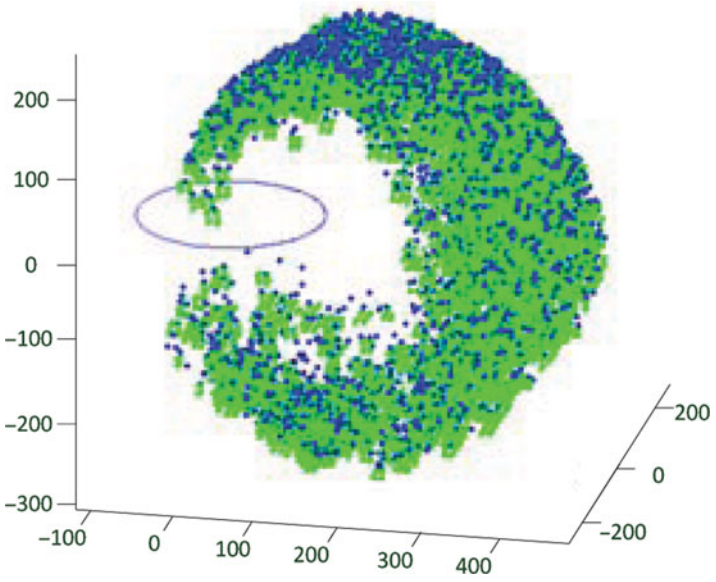

Fig. 4. Stable workspace with 5000 samples.

called force-closure:

$$Gf_c = \begin{bmatrix} 0 & 1 & 0 & 0 & 1 & 0 & 0 & 0 \\ 0 & 0 & 1 & 0 & 0 & 0 & -1 & 0 \\ 1 & 0 & 0 & 0 & 0 & 1 & 0 & 0 \\ -a & 0 & 0 & 0 & 0 & a & 0 & 0 \\ 0 & 0 & 0 & 1 & 0 & 0 & 0 & -1 \\ 0 & a & 0 & 0 & -a & 0 & 0 & 0 \end{bmatrix} \begin{bmatrix} f_{1x} \\ f_{1y} \\ f_{1z} \\ f_{1t} \\ f_{2x} \\ f_{2y} \\ f_{2z} \\ f_{2t} \end{bmatrix} = - \begin{bmatrix} F_{gx} \\ F_{gy} \\ F_{gz} \\ 0 \\ 0 \\ 0 \end{bmatrix},$$

$$G = \left[Ad^T_{g^{-1}_{oc1}} B_{c1},\ Ad^T_{g^{-1}_{oc2}} B_{c2} \right].$$

Considering the friction cone constraints:

$$\begin{cases} \mu^2 {f_{2z}}^2 \geq \dfrac{{F_{gx}}^2}{4} + \dfrac{{F_{gz}}^2}{4} & if\ F_{gy} \geq 0, \\ \mu^2 {f_{1z}}^2 \geq \dfrac{{F_{gx}}^2}{4} + \dfrac{{F_{gz}}^2}{4} & if\ F_{gy} < 0. \end{cases} \tag{4}$$

From equation (4), it can be seen that the normal contact stress should be sufficiently large to maintain a stable grasp.

Assume that $\theta = [\theta_{11}, \theta_{12}, \theta_{13}, \theta_{14}, \theta_{15}]$ in equation (1) are active joints and $\alpha = [\theta_{21}, \theta_{22}, \theta_{23}, \theta_{24}, \theta_{25}]$ are passive joints. Given θ, there exists α satisfying equations (2) and (3). The Monte Carlo method is used to approximate the workspace. The computer program picks a random sampling value for variable θ and then investigates the existence of appropriate α. The feasible values of θ and α are used to calculate the object position, and a dot is plotted on the screen for each feasible sample. The workspace with 5000 samples is shown in Fig. 4. We can evaluate the kinematic performances of the manipulator mechanism by analyzing the workspace characteristics and plan a manipulation trajectory by searching a continuous path in the workspace. Many algorithms, such as the A^* method and the artificial potential field method, have been published to accomplish this searching procedure.[24,25]

https://doi.org/10.1017/S0263574714001799 Published online by Cambridge University Press

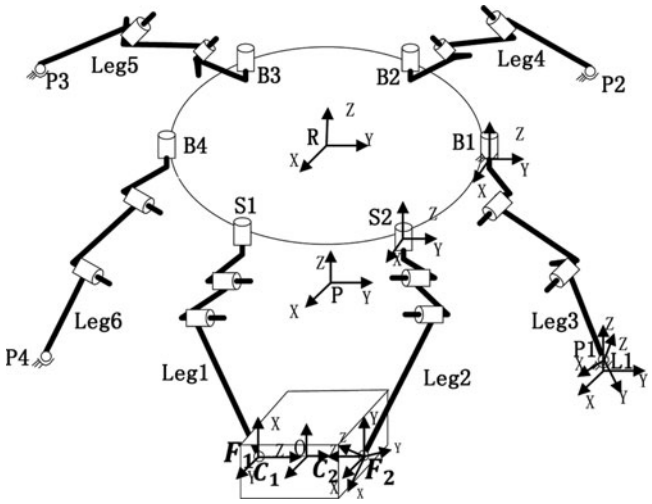

Fig. 5. Coordinate frames and parameters.

3.2. Kinematic analysis of the coordinated manipulation method

Leg motion is capable of increasing the manipulability by changing the stand positions of the legs or adjusting the postures of the body via bending and stretching of the legs. This leg motion is discussed as a coordinated manipulation method in this section. We assume that the leg tips that are in contact with the floor never slip. Without loss of generality, leg-1 and leg-2 are selected as target legs. The supporting legs and the hexapod body are considered as a parallel mechanism, and each target leg is regarded as a typical serial manipulator; thus, the entire hexapod robot can be considered as hybrid serial-parallel mechanism while it manipulates the object. As shown in Fig. 5, we define Σ_P as the universal coordinate frame attached to the ground, Σ_R as the body coordinate frame fixed on the body center, and Σ_O as the object frame fixed on the object center. For each target leg, $\beta_i = [\alpha_{i1}, \alpha_{i2}, \alpha_{i3}]$ represents the joint angles; we attach frame S_i to the base of the leg and frame F_i to the leg tip at the contact point. Note that the frame F_i moves with the leg tip, while the frame C_i, also located at the contact point, moves with the object. For each supporting leg, $\theta_j = [\alpha_{j1}, \alpha_{j2}, \alpha_{j3}]$ represents the joint angle, frames B_j are the base frames of leg j, frames P_j are located at the leg-end points, and frames L_j are at corresponding points on the ground (where, $i = 1 \ldots 2$, $j = 1 \ldots 4$). Assume that the contact locations are fixed on the object and the contact types are point contacts with friction. In this case, the constraints between the object and a leg tip can be formulated by requiring that certain velocities are equal. In general, the directions in which motion is constrained are precisely those in which forces can be exerted. Hence, for a contact with wrench basis B_{c_i}, we require that

$$B_{c_i}^T V_{f_i c_i}^b = 0. \tag{5}$$

Because all computations are performed with body velocities, we temporarily drop the superscript b for simplicity.

By decomposition of velocity in different frames, we find that

$$V_{f_i c_i} = Ad_{g_{pc_i}^{-1}} V_{f_i p} + V_{pc_i} = -Ad_{g_{pc_i}^{-1}} Ad_{g_{pf_i}} V_{pf_i} + V_{pc_i}, \tag{6}$$

where V_{pf_i} is the leg tip velocity relative to the universal coordinate frame, which can be decomposed as

$$V_{pf_i} = Ad_{g_{Rf_i}^{-1}} V_{pR} + V_{Rf_i}, \tag{7}$$

$$V_{Rf_i} = Ad_{g_{s_i f_i}^{-1}} V_{Rs_i} + V_{s_i f_i} = V_{s_i f_i} = Ad_{g_{s_i f_i}^{-1}} J_{s_i f_i}^s \dot{\beta}_i \tag{8}$$

https://doi.org/10.1017/S0263574714001799 Published online by Cambridge University Press

Because the contact frame is fixed relative to the object frame, it follows that

$$V_{pc_i} = Ad_{g_{oc_i}^{-1}} V_{po} + V_{oc_i} = Ad_{g_{oc_i}^{-1}} V_{po} \tag{9}$$

The body, supporting legs and the ground can be seen as the components of a 4-RRRS parallel mechanism that has 6 DOF. We assume that θ_{ij} are actuating joints ($i = 1, 2, 3; j = 1, 2$), while joints $\theta_{i,3}$ and $\theta_{4,i}$ are passive joints ($i = 1, 2, 3$). Considering the velocity constraints that $v_{l_j p_j} = 0$ and $V_{l_j l_m} = 0$, the Jacobian matrix of the parallel mechanism can be written as[26]

$$\begin{cases} J_X V_{pR} = J_a \dot{\theta}_a \\ J_1 \dot{\theta}_a = J_2 \dot{\theta}_p \end{cases}, \tag{10}$$

where $\dot{\theta}_a$ are the velocities of the actuating joints, and $\dot{\theta}_p$ are the velocities of the passive joints. It can be proved that the necessary and sufficient condition for matrix J_X to be full rank is that points P_1, P_2, and P_3 do not fall on a line. Hence, there is no forward singularity in this parallel mechanism kinematics. Substituting Eqs. (6), (7), (8), and (9) into Eq. (5) gives

$$B_{c_i}^T V_{pc_i} = B_{c_i}^T Ad_{g_{oc_i}^{-1}} V_{po} = G_i^T V_{po},$$

where G_i is the grasp map. Substituting the parallel mechanism kinematic relation into this equation yields:

$$B_{c_i}^T Ad_{g_{pc_i}^{-1}} Ad_{g_{pf_i}} V_{pf_i} = B_{c_i}^T Ad_{g_{Rc_i}^{-1}} J_X^+ J_a \dot{\theta}_a + B_{c_i}^T Ad_{g_{s_i c_i}^{-1}} J_{s_i f_i}^s \dot{\beta}_i.$$

Finally, the object velocity V_{po} and the velocity of each kinematic pair $[\dot{\theta}_a, \dot{\beta}_1, \dot{\beta}_2]$ are related as follows:

$$A[\dot{\theta}_a, \dot{\beta}_1, \dot{\beta}_2]^T = [G_1, G_2]^T V_{po}, \tag{11}$$

where

$$A = \begin{bmatrix} B_{c_1}^T Ad_{g_{Rc_1}^{-1}} J_X^+ J_a, & B_{c_1}^T Ad_{g_{s_1 c_1}^{-1}} J_{s_1 f_1}^s, 0 \\ B_{c_2}^T Ad_{g_{Rc_2}^{-1}} J_X^+ J_a, 0, & B_{c_2}^T Ad_{g_{s_2 c_2}^{-1}} J_{s_2 f_2}^s \end{bmatrix}.$$

Equation (11) shows kinematic relations for integrated arm and leg manipulation, which are the fundamental grasping constraints.

3.3. Optimization algorithm and control model

If the position and the orientation of the object, the locations of footholds, and the position and the orientation of the body are given, then from Eq. (11), we can obtain

$$J\dot{\theta} = \dot{x},$$

where $\dot{\theta}$ represents the velocities of the robot joint angles, and $\dot{x}$ represents the object velocity. The solution to this redundant equation can be formulated as

$$\dot{\theta} = J^+ \dot{x} + N\lambda,$$

where J^+ represents the pseudo-inverse of J, λ is an arbitrary joint velocity vector, and N is the null space of J, corresponding to a self-motion of linkages that does not move the end effector. We usually take $\lambda = 0$ for the attractiveness of the least squares property, which is adopted by Koyachi *et al.*[11] in his study of limb mechanism. However, this solution may cause the robot to overturn during manipulation; thus, we take static stability into consideration when seeking lower energy cost, and

https://doi.org/10.1017/S0263574714001799 Published online by Cambridge University Press

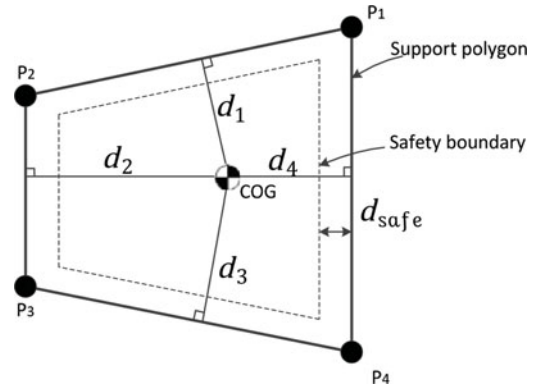

Fig. 6. Definition of safety margin.

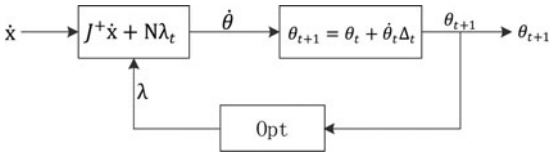

Fig. 7. Velocity servo control model.

the optimization problem is defined as

$$\text{Minimum}: f = \sum \dot{\theta}_t^T \dot{\theta}_t = \left(J^+\dot{x} + N\lambda_t\right)^T \cdot \left(J^+\dot{x} + N\lambda_t\right).$$

$$\text{Subject to}: \begin{cases} d\left(\theta_{t+1}\right) \geq d_{\text{safe}} \\ \theta_{t+1} = \theta_t + \dot{\theta}_t \Delta_t, \\ \dot{\theta}_t = J^+\dot{x} + N\lambda_t \end{cases}$$

where d_{safe} is the minimum safety margin, as depicted in Fig. 6. It is presumed that $\sum \dot{\theta}^T\dot{\theta}$ is approximately related to kinetic energy, which would be minimized by a pseudo-inverse solution. In addition, $d(\theta_t)$ is the static stability margin of the system defined as follows:

$$d\left(\theta\right) = \min\left(d_i\right) i = 1 \ldots 4,$$

$$d_i = \begin{cases} |d_i| \text{ COG is within the supporting polygon} \\ -|d_i| \text{ else} \end{cases}.$$

The above-described optimization is a typical quadratic optimization problem with linear constraints, which can be easily solved by using the Matlab software. Next, the optimal control model for integrated arm and leg manipulation is designed as shown in Fig. 7, where the Opt module represents the above-mentioned optimal method.

4. Simulations and experiments

To verify the proposed methods, we designed two contrasting scenarios for generating an identical object motion trajectory. In scenario A, the object is lifted using the basic manipulation method (presented in Section 3.1) and is then thrown out using the coordinated manipulation method (provided in Section 3.2) with the least squares solution. In scenario B, the object is lifted using the basic manipulation method (proposed in Section 3.1) and is then thrown out using the coordinated manipulation method with optimal solutions (proposed in Section 3.3). We expect to reveal the effectiveness and demonstrate advantages of our optimal method by the contrasting tests. The target object adopted is a 90 × 60 × 20 cuboid, with a weight of 1 kg, and the object mass center is

https://doi.org/10.1017/S0263574714001799 Published online by Cambridge University Press

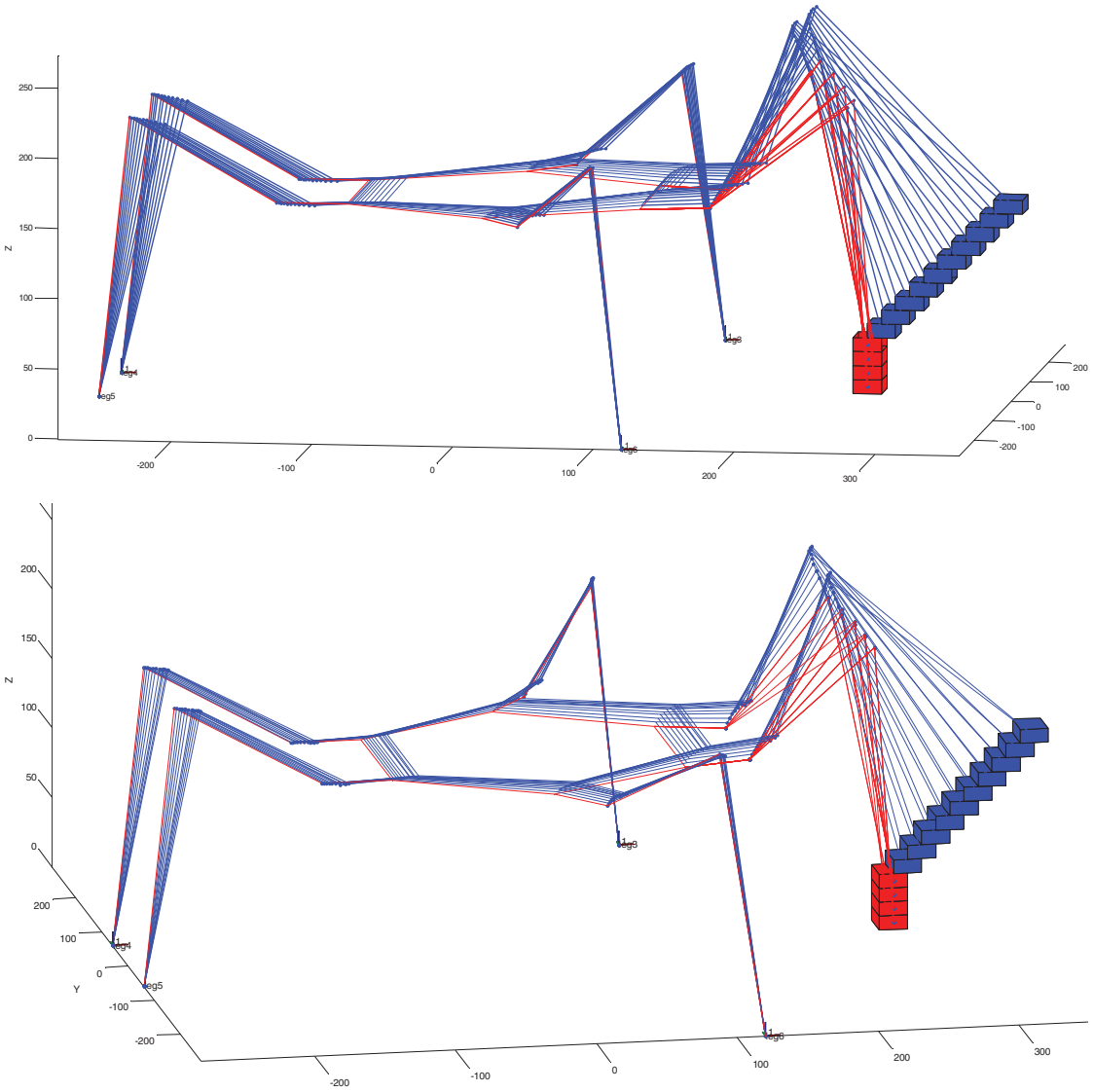

Fig. 8. Postures of the robot in (a) scenario A, and (b) scenario B.

initially located at the position O(260, 0, 10). The object is lifted at a constant velocity of 0.01 m/s along the z-axis in 3 s, and then thrown out at a constant velocity 0.017 m/s along the direction of 45° in the X–Z plane after that time. The robot body has a weight of 3 kg, and the body mass center is initially located at position R(0, 0, 140).The footholds are $P_1(120, 280, 0)$, $P_2(-140\sqrt{3}, 140, 0)$, $P_3(-140\sqrt{3}, -140, 0)$, $P_4(120, -280, 0)$.

Supposing that the center-of-gravity (COG) is only affected by the body and the object, the virtual manipulation model is established by using the Matlab software. The energy consumption index and the static stability margin of the robot are computed every 0.1 s. The simulation results are shown in Figs. 8–10. In Fig. 8, the postures of the robot in two scenarios are illustrated, where the lifting phase is displayed with the red color and the throwing phase is displayed with the blue color. Figure 8(a) indicates that the robot's body moves forward by a significant amount, and Fig. 8(b) indicates that the robot significantly rotates its body during the operation. In Figs. 9 and 10, the horizontal axis represents the time, and the vertical axis represents the energy consumption index and the COG position projected along the x-axis respectively; blue and red lines denote the values of scenarios A and B respectively. We found that energy consumption in the two scenarios is almost identical before 11 s, while the energy consumption in scenario B becomes higher after 11 s (Fig. 9). The extra energy consumed is used to maintain stability, with the robot rotating its body more in scenario B, which is

https://doi.org/10.1017/S0263574714001799 Published online by Cambridge University Press

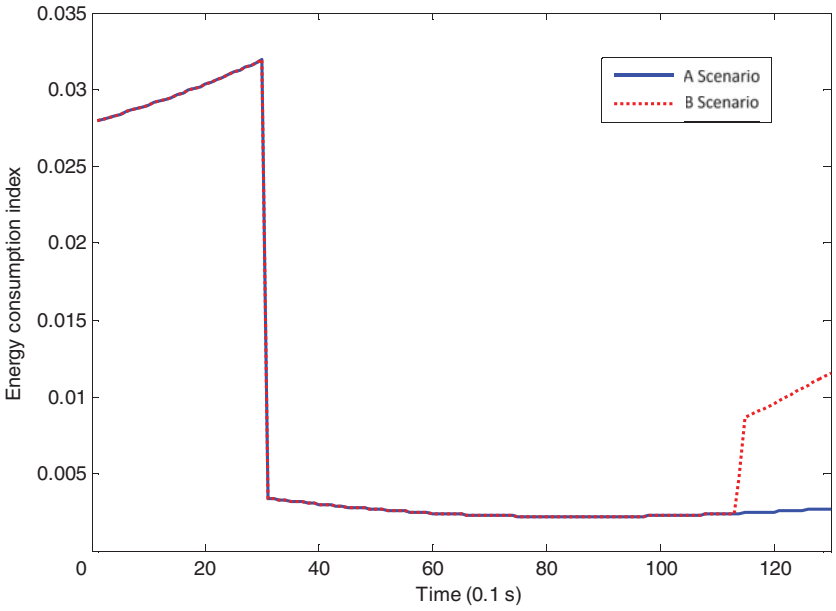

Fig. 9. Energy consumption criteria.

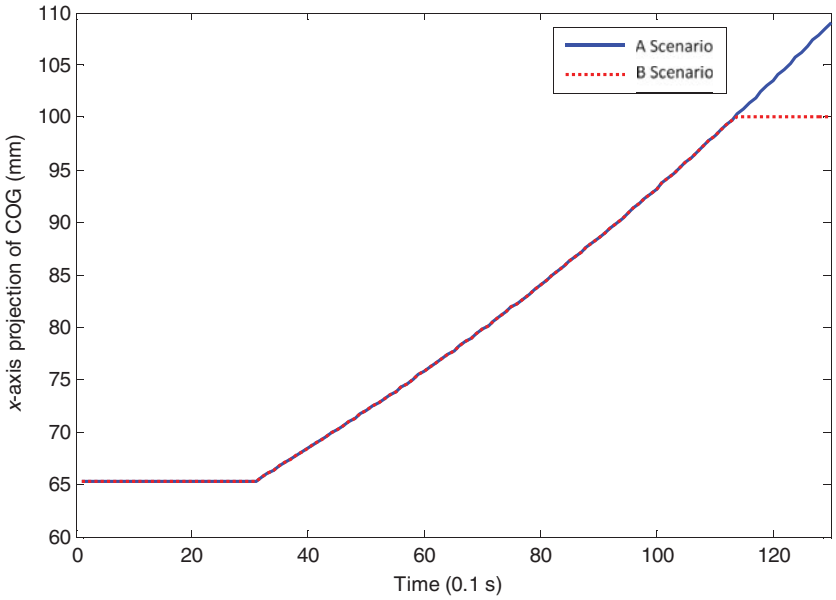

Fig. 10. Trajectories of the COG.

a very effective way to prevent the COG going beyond the supporting polygon (Fig. 8). The robot may overturn during the operation in scenario A.

Corresponding experiments were also performed on NOROS-III robots. Images of scenario A are presented in Fig. 11. A sequence demonstrating the effectiveness of the optimal method is shown in Fig. 12. White blocks are attached to the robot body and environments, which are taken as reference objects to indicate posture changes during manipulation; the distance between reference objects, marked as D in Figs. 11–12, is also measured. These data are analyzed and assigned fitting curves by the Matlab program, as illustrated in Fig. 13. The horizontal axis represents the time, and the vertical axis represents the distance between the reference objects. The marker points represent the distance at the moment when the images in Figs. 11–12 were taken.

According to experimental results, distance between the reference objects continues to increase during the throwing phase in scenario A, and the robot is overturned at the midpoint (Fig. 11d),

https://doi.org/10.1017/S0263574714001799 Published online by Cambridge University Press

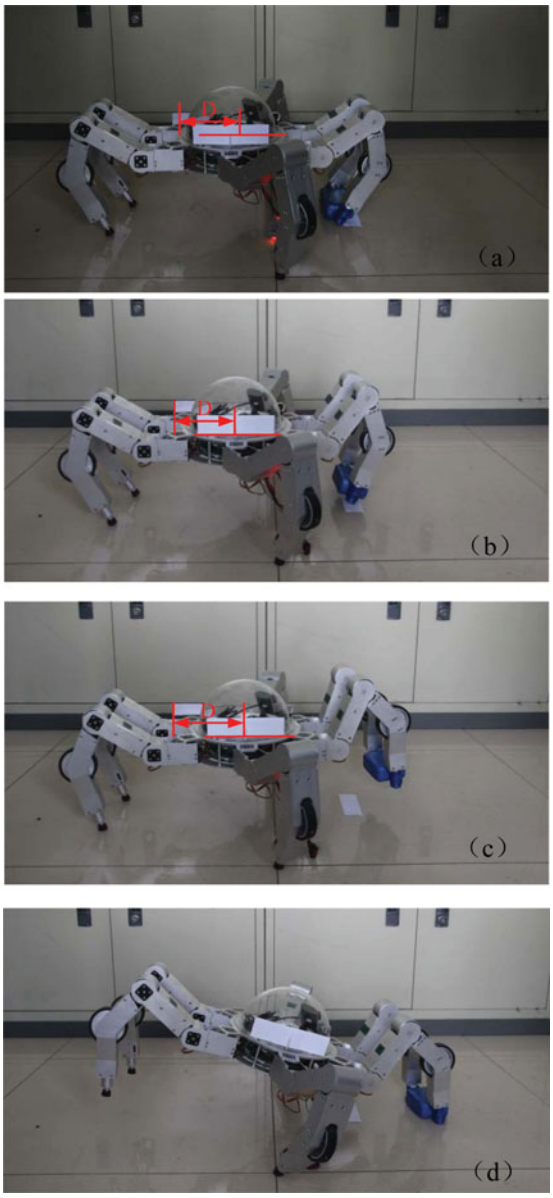

Fig. 11. Several postures of the robot in scenario A. (a)–(b) show the postures of the lifting operation. (c)–(d) show the postures of the throwing operation; the robot is overturned at the midpoint as shown in (d).

which contrasts with scenario B (Fig. 13). Scenario B indicates that the robot successfully adjusted its posture to throw out the object (Fig. 12e). The variation tendency (Fig. 13) of the distance between the reference objects agrees with the simulated changes of COG (Fig. 10). The robot configurations captured during the experiments (Figs. 11–12) coincide well with the simulation postures (Fig. 8). All these results strongly verify the algorithms proposed in this paper; therefore, we can conclude that the hexapod robot manipulation capability can be improved by using the methods provided.

5. Conclusions

In this paper, manipulation methods of hexapod robots were studied in detail and tested on a NOROS-III prototype. We presented two methods in which a hexapod robot uses its legs to manipulate objects. The first method is simple and effective for small range manipulations, and a stable workspace is also provided. The second method is more complex and has better performance in terms of

https://doi.org/10.1017/S0263574714001799 Published online by Cambridge University Press

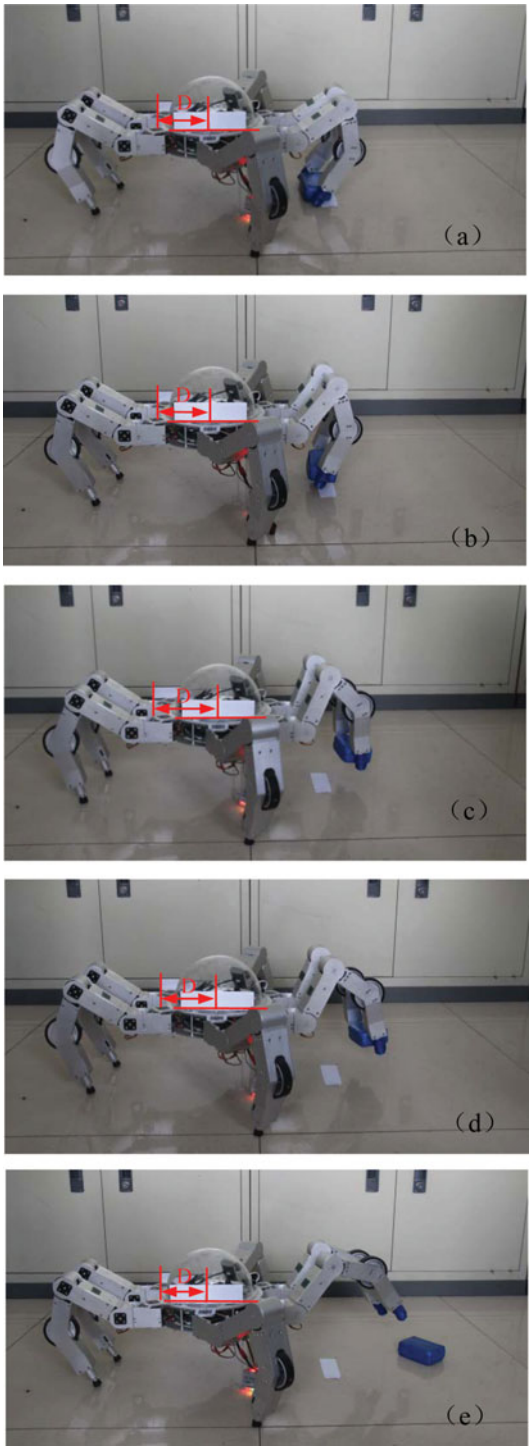

Fig. 12. A sequence of postures in scenario B, in which the hexapod lifts the object and throws it out successfully.

manipulability and stability. The kinematic model was built for a motion controller. By providing the energy consumption criteria and the static stability index, we found optimal solutions to the redundant kinematic model. The results presented in this paper contribute to the improvement of hexapod robots' manipulability. Possible applications of the proposed methods include the exploration of unknown environments, such as moon projects. Future works will be focused on the dynamic manipulation model, and the dynamic stability index will be taken into account to improve performance.

https://doi.org/10.1017/S0263574714001799 Published online by Cambridge University Press

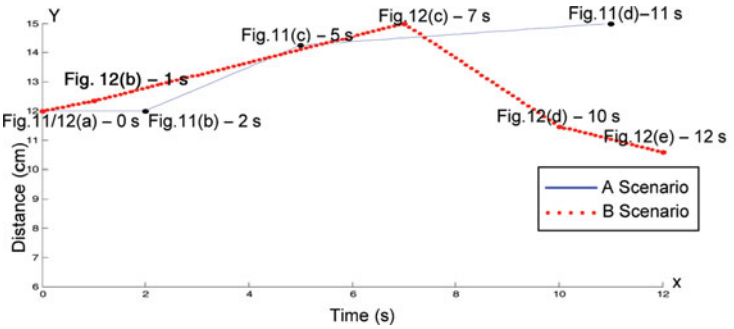

Fig. 13. Distances between the reference objects.

Acknowledgements

We acknowledge the support of the Key Scientific Cooperation Program of the China and Italy Governments (2006–2009) and the National Science Foundation for Distinguished Young Scholars of China (Grant No. 51125020). The previous prototypes NOROS-I and NOROS-II were developed cooperatively by Politecnico di Milano and the Beijing University of Astronautics and Aeronautics. We thank the joint research work of the Polimi and BUAA team involved in the development of the NOROS project.

References

1. S. Hirose, "Three Basic Types of Locomotions in Mobile robots," **In**: *Proceedings of the 5th International Conference on Advanced Robotics 1991, 'Robots in Unstructured Environments' (ICAR '91)*, Pise, Italy (Jun. 19–22, 1991) pp. 12–17.
2. A. Preumont, P. Alexandre and D. Ghuys, "Gait Analysis and Implementation of a Six-Leg Walking Machine," **In:** *Proceedings of the Fifth International Conference on Advanced Robotics 1991 'Robots in Unstructured Environments' (ICAR '91)*, Pise, Italy (Jun. 19–22, 1991) pp. 941–945.
3. X. Ding, Z. Wang, A. Rovetta and J. Zhu, "Locomotion Analysis of Hexapod Robot," **In**: *Climbing Walking Robots* (B. Miripour, ed.) (InTech, Rijeka, Croatia, 2010) pp. 291–310.
4. J.-M. Yang and J.-H. Kim, "Fault-tolerant locomotion of the hexapod robot," *Systems Man Cybern. IEEE Trans. Cybern.* **28**, 109–116 (1998).
5. Y. Yamamoto and X. Yun, "Coordinating locomotion and manipulation of a mobile manipulator," *IEEE Trans. Autom. Control* **39**, 1326–1332 (1994).
6. O. Khatib, K. Yokoi, K. Chang, D. Ruspini, R. Holmberg and A. Casal, "Vehicle/Arm Coordination and Multiple Mobile Manipulator Decentralized Cooperation," **In**: *Proceedings of the 1996 IEEE/RSJ International Conference on Intelligent Robots and Systems (IROS 96)*, Osaka, Japan (Nov. 4–8, 1996) pp. 546–553.
7. K. Kato and S. Hirose, "Development of the quadruped walking robot, TITAN-IX – mechanical design concept and application for the humanitarian demining robot," *Adv. Robot.* **15**, 191–204 (2001).
8. B. H. Wilcox, "ATHLETE: A Cargo and Habitat Transporter for the Moon," **In**: *Proceedings of the 2009 IEEE Conference on Aerospace*, Big Sky, MT, USA (Mar. 7–14, 2009) pp. 1–7.
9. B. H. Wilcox, T. Litwin, J. Biesiadecki, J. Matthews, M. Heverly, J. Morrison, J. Townsend, N. Ahmad, A. Sirota and B. Cooper, "ATHLETE: A cargo handling and manipulation robot for the moon," *J. Field Robot.* **24**, 421–434 (2007).
10. N. Koyachi, T. Arai, H. Adachi, K.-I. Asami and Y. Itoh, "Hexapod with Integrated Limb Mechanism of Leg and Arm," **In**: *Proceedings of the 1995 IEEE International Conference on Robotics and Automation (ICRA)*, Nagoya, Aichi, Japan (May 21–27, 1995) pp. 1952–1957.
11. T. Arai, N. Koyachi, H. Adachi and K. Homma, "Integrated Arm and Leg Mechanism and Its Kinematic Analysis," **In**: *Proceedings of the 1995 IEEE International Conference on Robotics and Automation*, Nagoya, Aichi, Japan (May 21–27, 1995) pp. 994–999.
12. N. Koyachi, H. Adachi, M. Izumi and T. Hirose, "Control of Walk and Manipulation by a Hexapod with Integrated Limb Mechanism: MELMANTIS-1," **In:** *Proceedings of the IEEE International Conference on Robotics and Automation (ICRA'02)*, Washington, DC, USA (May 11–15, 2002) pp. 3553–3558.
13. K. Inoue, Y. Nishihama, T. Arai and Y. Mae, "Mobile Manipulation of Humanoid Robots-Body and Leg Control for Dual Arm Manipulation," **In**: *Proceedings of the IEEE International Conference on Robotics and Automation (ICRA'02)*, Washington, DC, USA (May 11–15, 2002) pp. 2259–2264.
14. K. Bouyarmane and A. Kheddar, "Humanoid robot locomotion and manipulation step planning," *Adv. Robot.* **26**, 1099–1126 (2012).
15. K. Yoneda and S. Hirose, "Tumble Stability Criterion of Integrated Locomotion and Manipulation," **In**: *Proceedings of the 1996 IEEE/RSJ International Conference on Intelligent Robots and Systems (IROS 96)*, Osaka, Japan (Nov. 4–8, 1996) pp. 870–876.

16. U. T. M. Melaka, "Development of hexapod robot with manoeuvrable wheel," *Institutions* **49**, 119–136 (2012).
17. W. A. Lewinger, M. S. Branicky and R. D. Quinn, *Insect-Inspired, Actively Compliant Hexapod Capable of Object Manipulation* (Springer, New York, NY, 2006).
18. D. Belter and P. Skrzypczyński, "A biologically inspired approach to feasible gait learning for a hexapod robot," *Int. J. Appl. Math. Comput. Sci.* **20**, 69–84 (2010).
19. K. Inoue, K. Ooe and S. Lee, "Pushing Methods for Working Six-Legged Robots Capable of Locomotion and Manipulation in Three Modes," **In**: *Proceedings of the 2010 IEEE International Conference on Robotics and Automation (ICRA)*, Anchorage, Alaska (May 3–8, 2010) pp. 4742–4748.
20. R. M. Voyles and A. C. Larson, "Terminatorbot: A novel robot with dual-use mechanism for locomotion and manipulation," *IEEE/ASME Trans. Mechatronics* **10**, 17–25 (2005).
21. Z. Wang, X. Ding and A. Rovetta, "Analysis of typical locomotion of a symmetric hexapod robot," *Robotica* **28**, 893–907 (2010).
22. G. X.-H. HE Ping, Y. Lei, L. Hong and C. He-gao, "Multi- fingered manipulation with HIT/DLR hand," *J. Harbin Inst. Technol.* **37**(11), 1555–1559 (2005).
23. R. M. Murray, Z. Li, S. S. Sastry and S. S. Sastry, *A Mathematical Introduction to Robotic Manipulation* (CRC Press LLC, Boca Raton,
24. O. Khatib, "Real-time obstacle avoidance for manipulators and mobile robots," *Int. J. Robot. Res.* **5**, 90–98 (1986).
25. P. E. Hart, N. J. Nilsson and B. Raphael, "A formal basis for the heuristic determination of minimum cost paths," *IEEE Trans. Syst. Sci. Cybern*. **4**, 100–107 (1968).
26. I.-M. C. Anjan Kumar Dashy, S. H. Yeo and G. Yang, "Instantaneous Kinematics and Kinematic Control of In-Parallel Robots," *Proceedings of the Asian Conference on Robotics and Its Application* (Jun. 2001) pp. 7–12.

https://doi.org/10.1017/S0263574714001799 Published online by Cambridge University Press